Supporting Information

A Methods

All analytical expressions were obtained starting from Equation 3, the tQSSA approximation of the cycle, the derivation of which is discussed in Appendix C. The full mass action kinetics (MAK) description of the system (again, see Appendix C) was analyzed numerically to obtain the data used in all the plots. Therefore, although the analytical expressions depend on the validity of the tQSSA, the general results do not as they have been numerically verified on the full system.

To analyze the steady state behavior, the cycle equation (Equation 3) corresponding to each regime was set to zero to obtain $\overline{A}$ at steady state. The quasi steady state expression for the phosphatase-protein complex, obtained in the process of deriving Equation 3 was then used to translate this into the steady state output A (see Appendix D for details).

To obtain the dynamic response O Eq.3 was linearized about a chosen steady state level, assuming that the deviations in the input from its steady state level are small. The steady state level of the input for the four cycles was chosen such that the steady state output was about half-way to saturation, to allow the cycles to respond as much as possible. Choosing other steady state values where the slope of the steady state response curve is small would lead to little response. Particular care has to be placed in the ultrasensitive cycle, which has a very small range of inputs where its slope is non-zero, implying that this cycle needs to be finely tuned for it to transmit dynamic information.

All numerical analysis was done in Matlab, starting from the full MAK description of the cycle. The data in Figure 2 was obtained by setting the derivatives to zero and solving the resulting algebraic relations numerically. The data in Figures 5, 4 and S1 was obtained by numerically integrating the MAK equations for the given inputs using the $ODE23s$ Matlab function. Finally, the data in Figure 6 was obtained by integrating the MAK equations using the Runge-Kotta algorithm on inputs of the form $E_0(1 + a \sin \omega t_i + \eta(0, 1))$ where t_i is any time point in the numerical integration and $\eta(0, 1)$ is a normal random variable (with unit variance and zero mean). The code is available upon request.

B Equations for four regimes

Regime 1: both kinase and phosphatase are saturated : ultrasensitive

This regime was first identified [27], where its steady state behavior was analyzed. Equation 3 reduces to

$$\frac{d\overline{A}}{dt} = k_1\overline{E_1} - k_2\overline{E_2},$$

indicating that in this regime the signaling cycle effectively integrates the difference of its (scaled) input and a reference level specified by the (scaled) phosphatase level. When the difference maintains the same sign for long enough, it will become saturated at a low or a high output level, for a negative and a positive difference, respectively. This regime can be used in feedbacks

requiring time integration (integral feedbacks), such as the one proposed to operate in bacterial chemotaxis [62].

Regime 2: kinase saturated, phosphatase unsaturated : signal-transducing

Of the two new regimes that we characterize in this study, the one with a saturated kinase and unsaturated phosphatase (Figure 2B) is of particular interest. We refer to this regime as signal-transducing because, as discussed below, it is ideal for transmitting noisy time-varying signals. Equation 3 for this regime becomes

$$\frac{d\overline{A}}{dt} = k_1\overline{E_1} - k_2\frac{\overline{E_2}}{K_2 + \overline{E_2}}\overline{A},$$

which is linear in $\overline{A}$. This has several interesting implications. In particular, it implies that for slow inputs (relative to the cut-off frequency $k_2\overline{E_2}/(K_2 + \overline{E_2})$) the output $\overline{A}$ will simply be a scaled copy of the input. This property, that the output is a scaled but otherwise undistorted copy of the input, is unique amongst the four regimes of the signaling cycle, which combined with the fact that quickly varying inputs (noise) are filtered out make this regime ideal for the transmission of signals. Furthermore, the fact that this cycle is a linear system implies that pathways (or part of pathways) built of cycles in this regime become highly tractable mathematically since all the well-developed signals and systems techniques would apply to them. Available biochemical data and in vivo measurements argue in favor of this regime to be present in cell signaling cascades (see Discussion).

Regime 3: kinase unsaturated, phosphatase saturated : threshold-hyperbolic

The second new regime has an unsaturated kinase and a saturated phosphatase, and Equation 3 becomes

$$\frac{d\overline{A}}{dt} = k_1\frac{\overline{E_1}(\overline{S} - \overline{A})}{K_1 + \overline{E_1}} - k_2\overline{E_2}.$$

Its steady state output is zero for inputs below a threshold and then increases hyperbolically with increasing steady-state inputs.

Regime 4: both kinase and phosphatase unsaturated : hyperbolic

This regime was also first identified in [27] and exhibits a hyperbolic steady state response. Equation 3 becomes

$$\frac{d\overline{A}}{dt} = k_1\frac{\overline{E_1}(\overline{S} - \overline{A})}{K_1 + \overline{E_1}} - k_2\frac{\overline{E_2}\,\overline{A}}{K_2 + \overline{E_2} + \overline{A}}$$

for this regime.

C Derivation of Equation 3

We start with the mass action kinetics description of the reactions specified by Equations 1 and 2. There are six chemical species and three conservation relations (the kinase, phosphatase and

substrate protein are conserved), yielding a total of three variables. Letting C_1 (C_2) denote the concentration of the inactive (active) enzyme-substrate complex IE_1 (AE_1), we write down the mass action kinetics equations for the enzyme-substrate complexes and for the amount of active protein $\overline{A}$ yields

$$\begin{aligned}
\frac{d\overline{A}}{dt} &= k_1 C_1 - k_2 C_2 && (5)\\
\frac{dC_1}{dt} &= a_1\big[(\overline{S} - \overline{A} - C_1)(\overline{E_1} - C_1) - K_1 C_1\big] \\
&= a_1\big[C_1^2 - (K_1 + \overline{E_1} + \overline{S} - \overline{A})C_1 + \overline{E_1}(\overline{S} - \overline{A})\big] && (6)\\
\frac{dC_2}{dt} &= a_2\big[(\overline{A} - C_2)(\overline{E_2} - C_2) - K_2 C_2\big] \\
&= a_2\big[C_2^2 - (K_2 + \overline{E_2} + \overline{A})C_2 + \overline{E_2}\,\overline{A}\big], && (7)
\end{aligned}$$

where $\overline{S}$ denotes the total amount of substrate protein, a_1 and a_2 are the association rate constants of the two enzymatic reactions and K_1 and K_2 the Michaelis Menten constants.

To apply the tQSSA, we then hypothesize that the complexes have faster dynamics than the active protein and that they are always at equilibrium with respect to the active substrate protein. This allows us to substitute C_1 and C_2 in Equation 5 with the equilibrium values, which are in turn found by setting the left hand side of Equations 6 and 7 to zero and solving for the complexes.

So doing yields

$$C_1 = \frac{K_1 + \overline{E_1} + \overline{S} - \overline{A}}{2}\big(1 - \sqrt{1 - 4r_1}\big) \quad \text{and} \quad C_2 = \frac{K_2 + \overline{E_2} + \overline{A}}{2}\big(1 - \sqrt{1 - 4r_2}\big)$$

where

$$r_1 = \frac{\overline{E_1}(\overline{S} - \overline{A})}{\big(K_1 + \overline{E_1} + \overline{S} - \overline{A}\big)^2} \quad \text{and} \quad r_2 = \frac{\overline{E_2}\,\overline{A}}{\big(K_2 + \overline{E_2} + \overline{A}\big)^2}.$$

To further simplify the equilibrium expressions for the complexes, we approximate to first order in r_1 and r_2 (which is reasonable when $r_1 \ll 1$ and $r_2 \ll 1$), yielding the following expressions for C_1 and C_2:

$$C_1 = \frac{\overline{E_1}(\overline{S} - \overline{A})}{K_1 + \overline{E_1} + \overline{S} - \overline{A}} \quad \text{and} \quad C_2 = \frac{\overline{E_2}\,\overline{A}}{K_2 + \overline{E_2} + \overline{A}}. \qquad (8)$$

These expressions are finally inserted into Equation 5 to yield the signaling cycle equation (Equation 3).

In [32], R. Tzafriri describes in full detail how to obtain the same result for a single enzymatic reaction in a self-consistent manner. In particular, he finds conditions under which the complexes indeed reach equilibrium with respect to the substrate, and under which the first order approximation of the square root is valid. The same argument carries through for each enzymatic reaction in the signaling cycle. In particular, the tQSSA is expected to hold when

1. Either $K_1 + \overline{E_1} \gg \overline{S}$ or $K_1 + \overline{S} - \overline{A} \gg \overline{E_1}$, and

2. Either $K_2 + \overline{E_2} \gg \overline{S}$ or $K_2 + \overline{A} \gg \overline{E_2}$.

As these inequalities are better satisfied, the tQSSA describes the signaling cycle better. Similarly, whereas a Michaelis Menten approximation would be valid only at low enzyme concentrations, an inspection of the conditions above shows the tQSSA is also valid when the enzyme concentrations are high. The conditions we use to define the four signaling regimes of the cycle are consistent with the sufficient conditions for the validity of the tQSSA.

D Steady State

The output of the cycle is the amount of free active protein and may be found from the amount of active protein $\overline{A}$ and of active complex C_2, since $A = \overline{A} - C_2$. Analytic approximations to the steady state response of the signaling cycle may then be obtained by finding expressions for $\overline{A}$ and C_2. The former can be found by setting the left hand side of Equation 3 to zero and solving for $\overline{A}$, while the latter is taken to be $\frac{\overline{E_2}\,\overline{A}}{K_2+\overline{E_2}+\overline{A}}$ as discussed in the appendix above.

So doing for the four signaling regimes results in analytic expressions for their steady state responses. The case of the ultrasensitive regime, however, involves a slightly different method.

Regime 1: ultrasensitive

Setting Equation 3 to zero for this regime results in $k_1\overline{E_1} = k_2\overline{E_2}$, and since for this regime $C_2 \approx E_2$ then this indicates that $C_2 \approx \frac{k_1}{k_2}\overline{E_1}$. Numerical simulation indicates that as long as $\frac{k_1}{k_2}\overline{E_1} \leq \overline{E_2}$ the previous relation is accurate and furthermore that the switch output is zero. As the input increases beyond this point, C_2 quickly increases to its maximal value $\overline{E_2}$ (i.e., the phosphatase becomes fully saturated, while the level of free inactive protein decreases to zero and the inactive complex $C_1 \approx \overline{E_2}\frac{k_2}{k_1}$. Together, these observations imply that for $\overline{E_1} \leq \frac{k_2}{k_1}\overline{E_2}$ the output of the cycle is zero and $\overline{A} \approx C_2 \approx \frac{k_1}{k_2}\overline{E_1}$, and that for inputs above this level $\overline{A}$ quickly saturates at $\overline{S} - \frac{k_2}{k_1}\overline{E_2}$, and the output level is given by $A = \overline{S} - \big(1 + \frac{k_2}{k_1}\big)\overline{E_2}$. This implies that no matter how high the input is, the output of the ultrasensitive cycle will never equal the total amount of substrate protein unless there is no phosphatase.

Regime 2: signal-transducing

Setting Equation 3 to zero for this regime results in $k_1\overline{E_1} - k_2\frac{\overline{E_2}}{K_2+\overline{E_2}}\overline{A} = 0$, so $\overline{A} = \frac{k_1}{k_2}\frac{K_2+\overline{E_2}}{\overline{E_2}}\overline{E_1}$. At the same time $C_2 \approx \frac{\overline{E_2}}{K_2+\overline{E_2}}\overline{A}$ so that $A = \frac{k_1}{k_2}\big(\frac{K_2+\overline{E_2}}{\overline{E_2}} - 1\big)\overline{E_1}$. This linear relationship between the output and the input can not hold for high inputs because the output must be less than the total amount of substrate. We therefore expect the output to saturate when there is not free inactive protein, i.e., when $\overline{A} + C_1 \approx \overline{S}$. Since $C_1 \approx \overline{E_1}$ in this regime, the previous expression implies that the switch will saturate when $\overline{E_1} \approx \frac{\overline{S}}{1+\frac{k_1}{\omega_2}}$, where $\omega_2 = \frac{k_2\overline{E_2}}{K_2+\overline{E_2}}$. Evaluating the output at this input level yields the saturation value of the switch in this regime: $A = \big(1 - \frac{\omega_2}{k_2}\big)\big(\frac{\frac{k_1}{\omega_2}}{1+\frac{k_1}{\omega_2}}\big)\overline{S}$.

Regime 3: threshold-hyperbolic

Setting Equation 3 to zero for this regime results in $\omega_1(\overline{S}-\overline{A})-k_2\overline{E_2}=0$, where $\omega_1 = k_1\frac{\overline{E_1}}{K_1+\overline{E_1}}$. This implies that $\overline{A}\approx\overline{S}-\frac{k_2}{\omega_1}\overline{E_2}$ and since $C_2\approx\overline{E_2}$, that $A\approx\overline{S}-(1+\frac{k_2}{\omega_1})\overline{E_2}$. This approximation is not expected to hold at low inputs, where it blows up. Instead, at low inputs the free active protein is expected to be zero and $\overline{A}\approx C_2\approx\frac{\omega_1}{k_2}(\overline{S}-\overline{A})$ from the first expression in this subsection. Solving for $\overline{A}$ gives $\overline{A}\approx\frac{\omega_1}{k_2+\omega_1}\overline{S}\approx A$ for low inputs. This expression is expected to break as the input level reaches a level $\overline{E_1}^*$ where the expression equals $\overline{E_2}$. Above that input the first expression for $\overline{A}$ is expected to hold. Therefore, for inputs below $\overline{E_1}^*$ the output is approximately zero, and then increases hyperbolically as $A\approx\overline{S}-(1+\frac{k_2}{\omega_1})\overline{E_2}$.

Regime 4: hyperbolic

Setting Equation 3 to zero for this regime results in $\omega_1(\overline{S}-\overline{A})-\omega_2\overline{A}=0$, where ω_1 and ω_2 are as defined above. Therefore $\overline{A}\approx\frac{\omega_1}{\omega_1+\omega_2}\overline{S}$ and since $C_2\approx\frac{\omega_2}{k_2}\overline{A}$ then $A=\left(1-\frac{\omega_2}{k_2}\right)\frac{\omega_1}{\omega_1+\omega_2}\overline{S}$. The saturation level of this regime is obtained by evaluating the previous expression in the limit as $\overline{E_1}$ becomes infinite.

E Quantifying the Quality of the Four Regime Approximations

Taking extreme values of the kinase and phosphatase MM constants allows us to obtain the four signaling regimes previously discussed. However, the results obtained from these approximations apply reasonably well to a wide range of MM constants, and not only at the extreme. The quality of the approximation does increase, however, as the MM constants become more extreme. To demonstrate this we numerically solved for the steady-state characteristic of Equation 3 for a wide range of kinase and phosphatase MM constants and compared them to the characteristics of each of the four regimes. For each set of K_1 and K_2 values, we set the left hand side of Equation 3 to zero and solve for $\overline{A}$ and then subtract $\frac{\overline{E_2}\,\overline{A}}{K_2+\overline{E_2}+\overline{A}}$ as discussed in the section above to obtain A. We do so for a range of total kinase values K_t and for each, we compute the difference from the steady-state of each of the four regime steady states. We finally square these differences and compute their mean resulting in the mean squared error for each regime. In Figure 3 we show what we refer to a the relative error, the square root of the squared error normalized by the total substrate S_t. This figure again shows that the regime approximations are each approximately valid over a large part of a quadrant, covering almost the full K_1 versus K_2 space when combined.

F Dynamics

To find approximate analytic expressions for the response of the system to inputs of the form $\overline{E_1} = E_0(1+a\sin\omega t)$, we use small signal analysis. This method consists of linearizing the system about its steady state level, and further assuming that the input deviates from its steady state level by small amounts. Any results thus obtained are expected to be valid for small E_0a, although numerically we have observed that the results so obtained describe the system better

than they might have the right to when $E_0 a$ is not small. The method works as follows: First let the function $f(\overline{A}, \overline{E_1})$ (or just f for simplicity) denote the rate of change of $\overline{A}$ as described by Equation 3 (i.e., $\frac{d\overline{A}}{dt} = f(\overline{A}, \overline{E_1})$), and let $\overline{A}_{ss}$ be the steady state level of $\overline{A}$ when the input is constant and equal to E_0, so that $f(\overline{A}_{ss}, E_0) = 0$. Then define the deviations from steady state levels $\delta\overline{A} = \overline{A} - \overline{A}_{ss}$ and $\delta\overline{E_1} = \overline{E_1} - E_0 = E_0 a \sin \omega t$. Assuming the deviations are always small and Taylor expanding $f(\overline{A}, \overline{E_1})$ about the steady state levels then yields

$$\frac{d\delta\overline{A}}{dt} = g\delta\overline{E_1} - \omega_c \delta\overline{A}, \tag{9}$$

where $g = \frac{\partial f}{\partial \overline{E_1}}\big|_{(\overline{A}_{ss}, E_0)}$ is referred to as the gain and $\omega_c = \frac{\partial f}{\partial \overline{A}}\big|_{(\overline{A}_{ss}, E_0)}$ as the cut-off frequency. This equation is linear and may be solved for arbitrary inputs $\delta\overline{E_1}$ by one of the many useful techniques to work with linear differential equation (i.e., by Laplace transforms). In particular, when $\delta\overline{E_1} = aE_0 \sin \omega t$ and the initial condition is zero

$$\delta\overline{A} = aE_0 \frac{g}{\sqrt{\omega^2 + \omega_c^2}} \cos\left(\omega t + \tan^{-1}\left(\frac{-\omega_c}{\omega}\right)\right) + aE_0 g\omega e^{-\omega_c t},$$

where $\tan^{-1}$ denotes the inverse tangent. Here, we are only interested in twice the amplitude of the steady state oscillations in $\overline{A}$, from maximum to minima. These are evidently given by Equation 4, such that for frequencies smaller than the cut-off ω_c the oscillations are proportional to $\frac{g}{\omega_c}$ and oscillations for frequencies larger than ω_c decay as $1/\omega$.

Because the output of the system is $A = \overline{A} - C_2$, we need to translate these oscillations in $\overline{A}$ to oscillations in A. In the ultrasensitive and threshold-hyperbolic regimes, $C_2 \approx \overline{E_2}$ so the oscillations in A equal those in $\overline{A}$. In the hyperbolic and signal-transducing regimes, $C_2 \approx \frac{\omega_2}{k_2}\overline{A}$, so the amplitude of the oscillations in A is that amplitude of the oscillations in $\overline{A}$ multiplied by a factor of $1 - \frac{\omega_2}{k_2}$.

Regime 1: ultrasensitive

For the ultrasensitive regime we do not need to use the method above. This regime needs to be fine-tuned to transmit signals because, as evidenced by its steady state response curve, is only responsive to changes in the input close to its inflection point $\overline{E_1} = \frac{k_2}{k_1}\overline{E_2}$. Choosing E_0 by this expression Equation 3, for the dynamic input becomes $\frac{d\overline{A}}{dt} = k_1 a E_0 \sin \omega t$ which is identical to Equation 9 with a gain of k_1 and cut-off frequency of zero. This will not hold for small enough frequencies because then O would become infinite. Instead at some effective cut-off frequency, the oscillations will cover the full range of values that the ultrasensitive cycle may take. That is, the effective cut-off frequency satisfies $2E_0 a\frac{k_1}{\omega_c} = \overline{S} - \left(1 + \frac{k_2}{k_1}\right)\overline{E_2}$, where the right hand side is the saturation level of the cycle. Solving for ω_c in this expression yields the cut-off frequency in Table 3. The ultrasensitive regime is the only one that achieved oscillations that cover its full steady state response range, and where the (effective) cut-off frequency depends on the input amplitude a.

Regime 2: signal-transducing

Because Equation 3 for this regime is already linear in $\overline{A}$ and in $\overline{E_1}$, it already has the same form as Equation 9 with $g = k_1$ and $\omega_c = \omega_2$. Multiplying the gain by $1 - \frac{\omega_2}{k_2}$ to translate to oscillations in $\overline{A}$ gives the result in Table 3.

Regime 3: threshold-hyperbolic

Applying the method described above results in the expressions in Table 3 (These results are not expected to hold when the steady state input E_0 is below the regime's threshold and the output is zero). For simplicity though, we let $\omega_0 = \omega_1\big|_{(\overline{E_1}=E_0)} = \frac{k_1 E_0}{K_1+E_0}$, which turns out to be ω_c for this regime.

Regime 4: hyperbolic

Applying the method described above results in the expressions in Table 3, where the cut-off turns out to be $\omega_c = \omega_0 + \omega_2$.

G Low-pass filtering

Figure S1 summarizes the low-pass filtering behavior for the four regimes. It shows O (color coded) versus a and ω (i.e., a horizontal cut through this plot would simply be an O versus ω curve such as those shown in Fig. 5). Some salient features are evident in this figure. (i) All regimes act as low-pass filters. (ii) Although Equation 4 is obtained using a small signal approximation and is expected to hold for small a, it provides a good guide for describing O for all values of a. Perhaps the biggest discrepancy is the fact that O does not increase linearly with a but saturates (see Fig. S1A,C,D). The signal-transducing regime, however, does seem to have a response that increases linearly with a so for a given frequency an input with twice the amplitude of another will result in twice the output O. (iii) Finally, for all regimes except the ultrasensitive regime (Fig. S1D) the response starts decreasing at about the same frequency, independent of a, where as for the ultrasensitive cycle smaller a results in smaller cut-off frequency.

The ultrasensitive regime

The ultrasensitive cycle is the only cycle that oscillates between a level close to its saturation value and zero for a wide range of inputs (red region of Fig. S1D). The cutoff frequency of this cycle is a function of both the total substrate protein of the cycle, and of the input's amplitude, a unique property of this cycle. For all other cycles, the cutoff frequency is independent of total substrate and of the input parameters.

The signal-transducing regime

The cutoff frequency depends only on the phosphatase level and phosphatase parameters, but the gain depends on both phosphatase and kinase parameters. Thus the cutoff frequency can be

tuned by changing phosphatase parameters or level, and the gain can be independently adjusted by changing the catalytic rate of the kinase via evolution.

The threshold hyperbolic regime

The cutoff frequency depends only on the average kinase level and kinase parameters. Thus the cutoff frequency may be tuned by changing the kinase level and/or parameters, and the gain may be tuned independently by adjusting phosphatase levels or parameters.

The hyperbolic regime

This cycle has a cutoff frequency that depends on both the kinase and the phosphatase. Increasing either one increases the cutoff frequency. The gain also depends on both the kinase and the phosphatase, so adjusting their levels will modify both the gain and the cutoff frequency of the switch.

H Supplementary Figures

Figure S1. Magnitude of the oscillations in the output as a response to oscillations in the input about a background kinase level. Plots **A, B, C** and **D** show the output oscillations O of the hyperbolic, signal transducing, threshold-hyperbolic and ultrasensitive switches, respectively (normalized by the steady-state saturation value of each cycle), shown in Figure 2, in response to an input of the form $\overline{E_1} = E_0(1 + a \sin wt)$. The magnitude of O is color coded and shown as a function of the input amplitude a and frequency ω. Output oscillations increase with increasing a and decrease with increasing ω as expected. The four cycles, however, respond very differently to their inputs. The parameters used for the cycles are the same as those in Figure 2, and $\overline{E_2} = 50\ nM$ except for the threshold-hyperbolic switch, where $\overline{E_2} = 100\ nM$.

Fig.S1

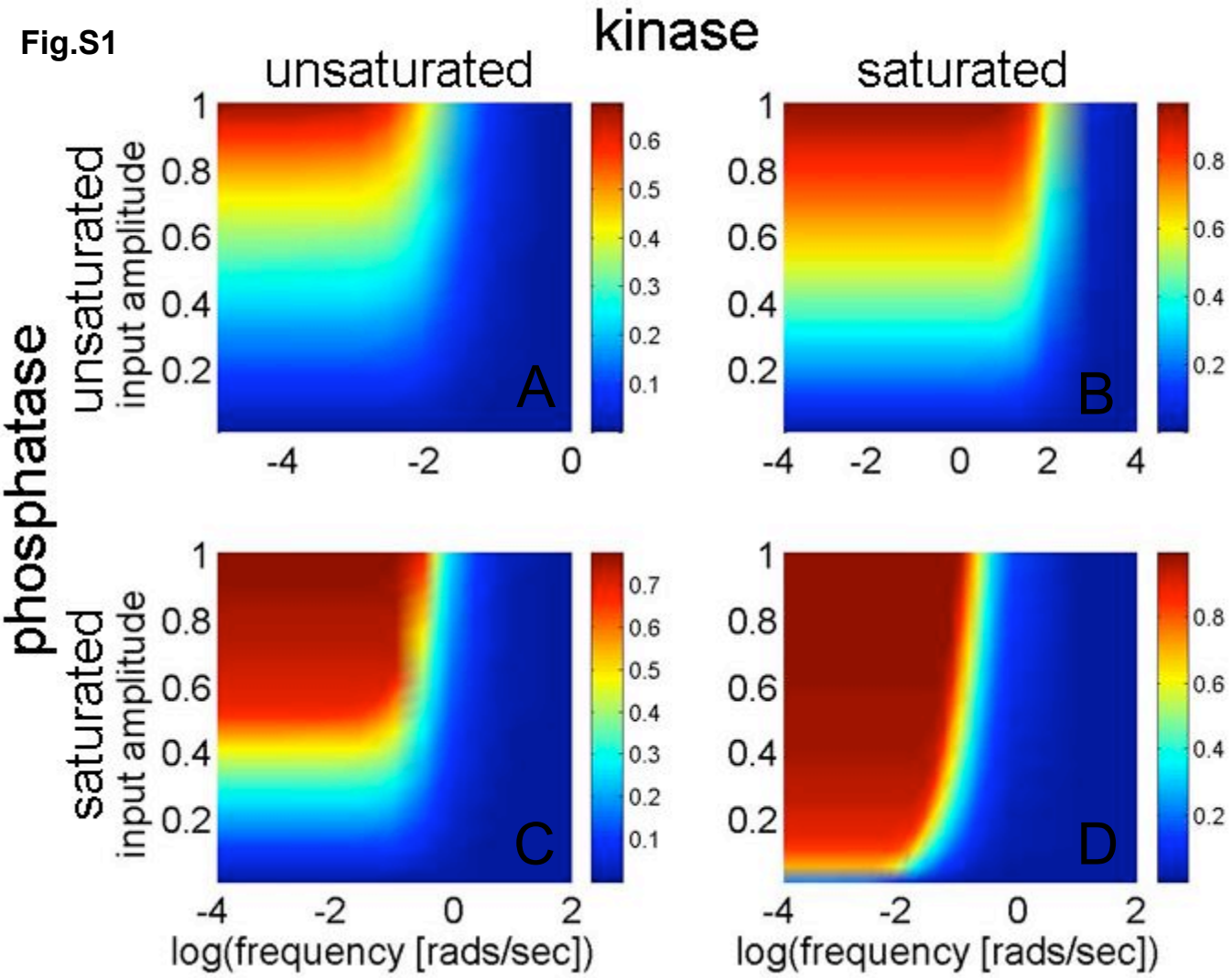
kinase
unsaturated
saturated
phosphatase
unsaturated
input amplitude
saturated
input amplitude
A
B
C
D
log(frequency [rads/sec])
log(frequency [rads/sec])